Answer to the review of Olivier Galland

Dear Olivier Galland,

Thank you very much for your thorough review and critical comments. Incorporating corrections accordingly to your suggestions will strongly improve the quality of the manuscript. Below we answer to your individual comments in detail and provide changes made.

Kind regards,

Michael Kettermann and colleagues

1. *Reproducibility of the results with respect to initial conditions. Figure 10 shows complex trends of the results. In particular, the authors argue that the lack of trend for the JF---Angle between 0 and 8 is possibly an effect of the limited width of the deformation box, as in experiments with small joint---fault angles joints do not necessarily intersect the basement fault trace. This is critical, because the authors implicitly imply that according to the initial conditions, i.e. the position of the joints with respect to the basement fault trace, the results are not reproducible. This means that the initial positions of the joints with respect to the basement fault trace is a very critical factor. And I suspect that it might be also the case for JF-angles larger than 8 degrees. Indeed, depending on the positions of the joints, a different number of joints can intersect the basement fault trace. This fact strongly questions the relevance of the trends of Figure 10. At least, this critical initial condition likely explains the very scattered and chaotic results displayed in Figure 10. The authors should really discuss, and even quantify, the effect of the initial position of the joints with respect to the basement fault trace. I suspect that this would require other laboratory tests to be performed.*

→ This is a very good comment. We looked into this and found that in fact the influence of the discussed initial conditions is not as strong as suspected. With a JF-angle of 0° the initial position of the joints only becomes critical for very large joint spacings, while in the presented geometry the fault truncates the joints at every possible position. The 4° JF-angle is in fact critical since the possible number of JF intersects can be 0 or 1 depending on the initial position. A substantially wider box would result in intersections and possibly the formation of stepovers. This cannot be represented in our data. However, at and above JF-angles of 8° the geometry always provides at least two intersections, independent of location of the joints with respect to basement fault. This means that we can always observe joint-fault interaction at two independent points, and we argue that the presented values are thus representative. However, the reviewer is right with stating that data in the range 0°>x°<8° cannot be interpreted without further consideration, at beast with data derived from experiments in a wider box.

However, while we certainly note a scatter of the measured data, we disagree with the statement of chaotic data. All data except the damage zone width show a general increasing trend. The decrease in damage zone width with higher JF-angles is interpreted to be the result of a gradual reduction of the influence of joints on the fault trace. At high JF-angles it is easier for the fault to fracture the intact material than to deviate far from its preferred orientation while following the joints. We modified the manuscript accordingly. Section 4 now reads ***:***

"Our quantitative analyses show an increase of all analyzed attributes from small to large JF-angles for angles larger than 8° (Fig. 11). Initial positions of the joints with respect to the basement fault may be important for small JF-angles. In our experimental setup joint spacing is close enough so that the master fault underlies several joints. Hence the influence of joints on fault evolution at 0° may be interpreted quantitatively. However, position of joints with respect to master fault for the 4° JF-angle experiment may be inconclusive due to insufficient cross-cuttings between the joints and the master fault. The possible number of JF intersects can be 0 or 1 in our deformation box depending on the initial joint position. A substantially wider box would result in one or more intersections and consequently formation of step-overs. This cannot be represented in our data due to limited box width. However, at JF-angles of 8° and higher, at least two intersections between master fault and joint occur, independent of the initial location of the joints with respect to basement fault. This implies that we can always observe joint-fault interaction at at least two independent points, and results may be interpreted quantitatively."

We added the following paragraph to section 5.1 to discuss the development of the damage zone width:

"We note, that the damage zone width decreases for JF-angles larger than 16°. We interpret this to be the result of a reduced influence of the joints on the fault trace. At high JF-angles it is easier for the fault to fracture the intact material than to deviate far from its preferred orientation while following the pre-existing joints. However, although the damage zone is narrower the number of joints that are connected via the main fault is increasing."

2. *Initial conditions. The heights of the joints are of 5 cm, with respect to the 19 cm thick box. What is the effect of the ratio between the heights of the joints and the total thickness of the box? What would happen if, for example, the joints are as deep as half of the box? This has major consequences, as joints often fully cross cut rock layers entirely. I suspect that the results would be very different. The authors should also discuss this very important initial condition and it potential effect on their results. I recommend the authors to perform a few experiments with varying heights of the pre---existing joints.*

→ We agree, that there is much potential for investigating different geometries and we did not clearly discuss our choice. In our experiments, joint depth was scaled approximately to observations in CLNP (REF). Gypsum is only able to support open fractures up to a depth of 7 cm, below that depth joints will close because gypsum fails in shear under its own weight. This has been tested (van Gent reference). It is therefore not possible to test the effect of joints that cut the entire rock column in this setup, even though the idea is exciting. Further parameter studies investigating the effects of joint spacing or joint depth are certainly interesting but don't fit the scope and time-frame of this publication and will be part of future work. We added a paragraph on this in the new version of the manuscript, now reads …

"For example a model height of 19 cm represents approximately 600 m of sandstone in nature with a cohesion of 70 MPa. Our model geometry was scaled approximately to the joint and graben system of Canyonlands National Park, where ~100 m deep vertical joints cut through nowadays 400-500 m brittle sediments before faulting (McGill and Stromquist (1979); i.e. 5 cm joints in a 19 cm powder column). The material properties limit the testing of increasing joint depths. The hemihydrate powder fails under its own weight in shear in a depth of about 7 cm (van Gent et al., 2010). It is hence not possible to test the influence of joints cutting the entire 19 cm hemihydrate column. However, smaller joint depths may influence fault evolution. A thorough analysis of this effect would require extensive experimental series, testing different fault depths at different angles. This is beyond the scope of this study, and we leave analysis of different materials as well as different joint depths for future work."

3. *Section 5.3, Field data. This section is difficult to read, as there is no graphic support, i.e. no figure. The only figure is a field photograph, where none of the conclusions of the laboratory study is visible. This is incompatible with the conclusion of the authors that states "Robust structural features that occur in the models as well as in field prototypes…". In this paper, it is impossible to assess the relevance of the laboratory results with respect to field data. I thus would recommend the authors to include a figure (at least) displaying field data, such that the comparison between laboratory and field results is more obvious.*

→ We completely revised this paragraph according to the suggestions of the reviewer. First, we point out better limitations of comparison between model and nature, as natural examples are commonly more complicated due to potential multiple deformation events associated with stress field rotations. However, the comparability is striking in several regards. In addition to the field picture showing that similar structural inventory exists in CLNP and the analogue models (Figure 8), we now illustrate the inferences we made by two separate figures. First we provide airborne photographs from examples covering a range of JF-angles to illustrate the remarkable geometric similarity between experiments and natural example. Secondly, we compare elevation profiles of an experiment and an example in Devil's Lane (Canyonlands NP) where we demonstrate that both experienced progressive migration of fault activation from footwall to hanging wall, always reactivating existing joints. Section 5.3 now reads:

"Our results have direct implications for our understanding of natural dilatant fault systems in jointed rocks. The inherent complexity of naturally fractured rocks however, makes it difficult to transfer all observations made in the lab to one particular outcrop. The best natural example that we also chose as base for the scaling of our experiments is the Grabens area of the Canyonlands National Park, Utah, USA, which is an archetype for dilatant faults in jointed rocks (e.g. (McGill and Stromquist, 1979; Moore and Schultz, 1999; Rotevatn et al., 2009). The northern part of the Grabens is characterized by prominent vertical joint sets, which are older than the formation of the dilatant faults (McGill and

Stromquist, 1979; Schultz-Ela and Walsh, 2002). The most prominent joint set consists of up to several 100s of m long joints cutting through the upper 100 m of sandstone and roughly follows a NNE-SSW striking arcuate geometry of the graben bounding faults. The Grabens of Canyonlands National Park developed as an extensional fault array on top of a deforming layer of evaporites. Faults dip at 60° - 80° below the jointed layer (Kettermann et al., 2015; McGill and Stromquist, 1979; Moore and Schultz, 1999), comparable to our model setup. Angles between this joint set and fault strikes inferred from local trends range between 0° and ~25° (Kettermann et al., 2015), which is the range covered in our experiments.

The following structural elements observed in the experiments are also present and common in the field. Where joints are at an angle with respect to the orientation of the grabens, i.e. not normal to the regional direction of extension, faults step over from one joint to another forming the typical zigzagged shape (cf. Fig. 7D). Airborne imagery (Utah Automated Geographic Reference Center, 2009) of three selected areas shows different JF-angles and the resulting step-over geometries (Fig. 14). As in the experiments the distance between step-overs increases from small JF-angles (Fig. 14b) to larger angles (Fig. 14D).

The graben walls are surfaces of pre-existing joints at which the faults localize (Kettermann et al., 2015). Comparable to the models, in the field we infer a progressive migration of the graben bounding faults towards the foot wall by reactivating several pre-existing joints before a steady master fault forms. This is expressed by minor displacements reactivating some joints in the footwall, before eventually a stable master fault forms and accumulates most offset. Figure 15 shows elevation profiles of the 0° JF-angle experiment (Fig. 15a, derived from photogrammetry) and a location with 0° JF-angle in Devil's Lane (Fig. 15b, location marked in Fig. 14a by red star; National Elevation Dataset (NED) courtesy of the U.S Geological Survey). Both show the same stair steps formed by faults reactivating pre-existing joints with increasing displacement from east to west before the main graben-bounding fault formed.

As graben walls are vertical and faults dip shallower at depth, open fissures form at reactivated joints. In the field these are mostly filled with rubble and Quaternary sediments but at numerous locations sinkholes resulting from dilatational faulting exist where sediment and rainwater are transported into the subsurface (Biggar and Adams, 1987; Kettermann et al., 2015). Ground penetrating radar studies (Kettermann et al., 2015) suggest that the hanging-walls of the graben-bounding faults (i.e. the graben floors) are faulted as well, which is in agreement with the observations of our models. This shows that our models are capable of correctly reproducing the characteristic features observed in similar natural settings, allowing us in turn to make predictions of natural fault systems from these models. For example, our models suggest, that along the graben-bounding faults in the subsurface interconnected fluid pathways exist, that are partially filled with uncemented, coarse grain sediments and rubble.

However, there are limits to the comparability of our experiments and the Grabens fault system. In Canyonlands National Park a second set of pre-existing joints exists which is oriented roughly orthogonal to the NNE-SSW striking joint set. This joint set is parallel to orientation of the developing secondary fractures observed in our analogue experiments. As a result we are not able to compare formation and extent of secondary fractures observed in the models with structures in CLNP. Likewise, the exact position of step-over geometries may be affected, as they localize at and reactivate early formed secondary fractures. The existence of step-overs is however unquestionable, as they are elemental features in areas where faults interact with jointed rocks (Myers and Aydin, 2004).

…"

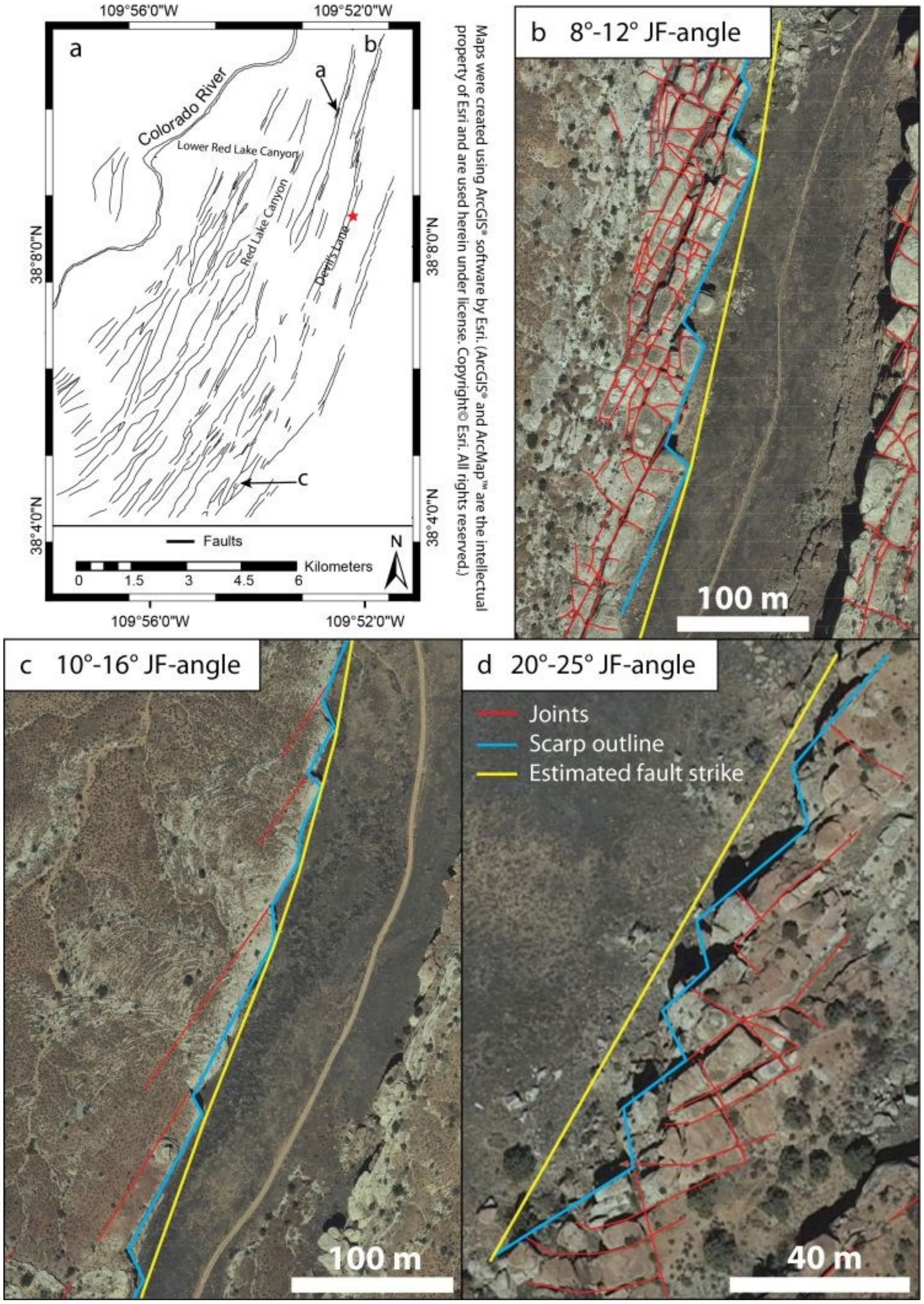

Figure 14: Collection of airborne photographs with interpretations of joints (red), estimated fault strike (yellow) and scarp outline (blue) of selected areas in Canyonlands National Park. a: Fault map of the Grabens of Canyonlands NP. Locations of b, c and d are shown as well as Fig. 15d.North is up in all images. b: 8°-12° JF-angle. c: 10°-16° JF-angle. d: 20-25° JF-angle.

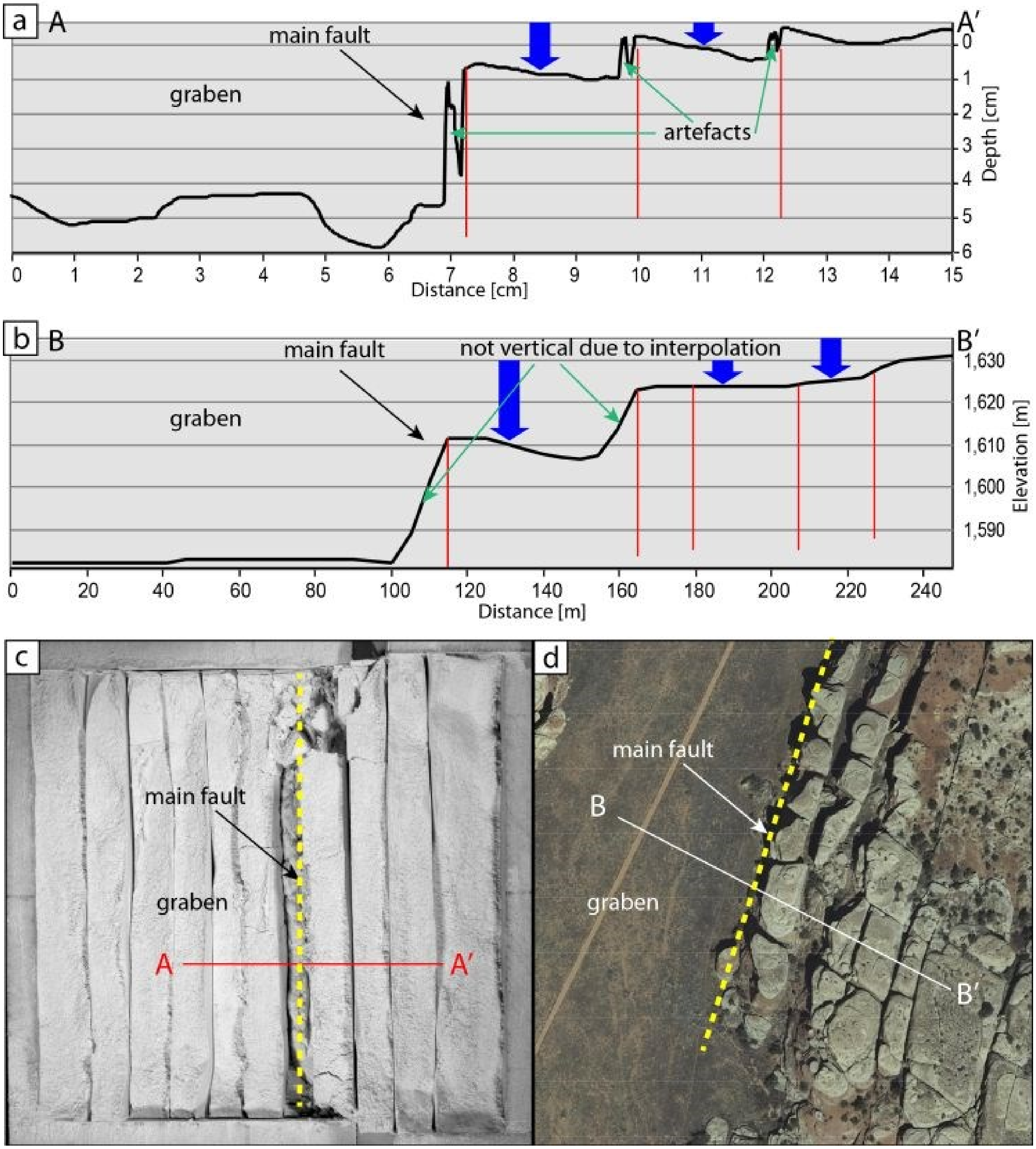

Figure 15: Comparison of elevation profiles from experiment (a) and nature (b). Both show typical stair step geometry caused by incremental reactivation of joints by fault migration from footwall to hanging-wall. Location of the profiles shown in c and d for experiment and nature, respectively. Location of d marked in Figure 14a by red star. Sharp spikes in elevation in a are artefacts of photogrammetric 3D reconstruction caused by shadows in open gaps. Inclined slopes in b instead of vertical surfaces result from interpolation of the elevation model. In reality these are vertical joint surfaces (cf. Kettermann et al., 2015).

Page 3, line 6. The authors could also include references to Galland et al. (2006), Galland et al. (2007) and Le Corvec et al. (2013) at the end of the last sentence of the paragraph.

→ Agreed and done.

Page 5, lines 7---18. The authors should specify whether the optical distortion is corrected or not. This has important implications on angle measurements presented later. Also they should indicate the lens characteristics, especially focal length, such that the reader has a good idea of the amount of optical distortion to be corrected.

→ This is a good point. The optical distortion was corrected using validated lens distortion correction profiles provided by Adobe, so that the image analyses are not compromised by that. We add a table summarizing lens types and focal lengths for each experiment and add the following sentence to the text to clarify:

"We use the top view photographs for PIV analysis (shot with the Nikon D90), to identify areas of the model at which deformation localizes, and calculate the displacement fields. All images are corrected for lens distortion using verified lens distortion profiles that are included in the Adobe CameraRaw software, so that later analyses are not compromised by distortion. Details on the used lenses and focal lengths are given in Table 1."

Section 3. In general, it lacks lots of references to figures. It is difficult to follow the text. Therefore, almost for each statement of the text, the authors should refer to the corresponding figure.

→ Agreed. We added some more references to corresponding figures to improve the clarity.

Page 7, last sentence. I don't understand the sentence. Maybe I am not awake, but the structure seems quite complicated. It would be good to split the sentence into several.

→ We agree that this paragraph is phrased confusingly and rephrased to:

"At the pre-cut bounding walls the 60° basement fault angle is enforced on the powder column by friction, hindering the formation of deep grabens. In the center of the box, however, the fault develops freely with a steep main fault, which causes the formation of deeper grabens. This

resulting subsidence-gradient, with shallow grabens at the sides and deeper grabens in the center of the experiments, produces a space-problem which results in the formation of reverse faults."

Page 7, lines 26---27. The authors mention that the y---displacement components highlight reverse faults. This is the case because the y---axis is coincidently properly oriented with respect to the local shortening. In addition, without the drawings of the authors, the reader would likely not see the reverse faults. In general, it is better to compute the divergence of the displacement field: positive divergence means extension, negative divergence means compression (Byrne et al. 2015). I recommend the authors to plot the divergence field to highlight the local compression.

→ This is of course not coincidentally, but we chose to plot the y-axis displacement to point out the reverse faults because it is parallel to the faults. However, you are right, a divergence plot would be better to show the local shortening. Unfortunately, due to the low deformation rates it is not possible to see the reverse faults in divergence plots of successive images (they are lost in the background noise), and in divergence plots of the summed up vector field they appear quite diffuse as well. I propose a compromise by creating a new figure showing a divergence plot of the summed up displacement field, y-component (Figure 8b) and the corresponding raw photo in order to provide maximum information to the reader. The text now reads:
"As the reverse faults form from bottom to top and do not necessarily propagate to surface, the related surface expression is difficult to see in photographs. Figure 9 provides a compilation of a top-view photograph (25° JF-angle at 95% displacement; Fig. 9a), a PIV analyses displaying the y-component of the displacement field, which is roughly parallel to the formed reverse faults (Fig 9b), and a PIV image showing the divergence of the displacement field which clearly shows locations of compression that indicate to reverse faulting (Fig. 9c). To clearly see the formation of the reverse faults, the reader is referred to the corresponding top-view movie (DOIXYZ!!!)."

Movies will be published as one dataset with one DOI using Pangea Data Publisher for Earth & environmental Science. We added the following sentence to the text and updated further references:
"Movies produced from image series of all experiments and the respective PIV images are freely accessible at https://issues.pangaea.de/browse/PDI-11894"

The data publishing is however still in progress. Until the videos are finally published with open access with an assigned DOI (which will be the case for the final version of the manuscript) the videos can be found here: https://rwth-aachen.sciebo.de/index.php/s/adccOLuVPT2dk63

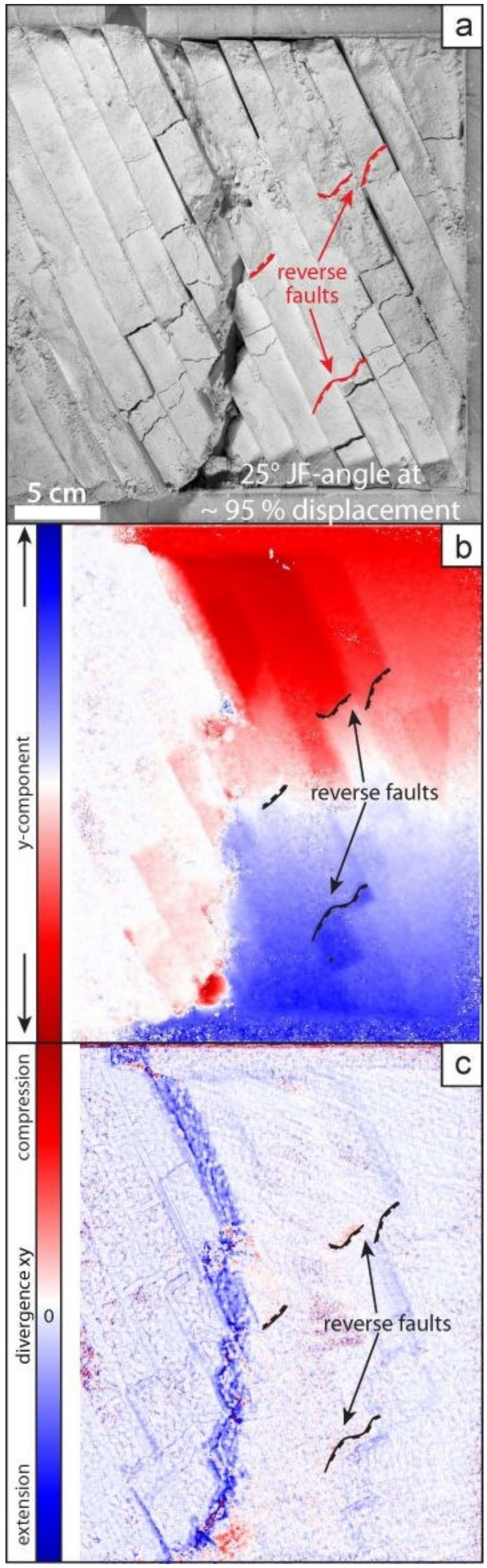

Figure 9: (a) Reverse faults marked in top-view photograph of experiment with 25° JF-angle at 95% displacement. (b) PIV image displaying the y-component of the displacement field. Sharp changes in color intensity indicate compression or dilation. (c) PIV image showing the divergence of the displacement field. Red colors show areas of local compression, i.e. reverse faulting.

Figure 12. What is actually plotted in this figure? Shear strain, divergence, rotation angle? This must be specified.

→ We redrafted the figure using divergence data and clarified in the caption: **"PIV images series of the 12° JF-angle experiment showing divergence of the displacement field** (extension: blue; compression: red)**. Note how different joints are reactivated at different stages of deformation."**